Research Square

Preprints are preliminary reports that have not undergone peer review.
They should not be considered conclusive, used to inform clinical practice,
or referenced by the media as validated information.

Systematic Design of Wideband Single-Layer Microstrip 180° Hybrid Couplers Using a Novel Topology

Parisa Safaei
Yazd University
Masoud Movahhedi
movahhedi@yazd.ac.ir

Yazd University

Research Article

Keywords: in–phase, microstrip–slot transition, Wilkinson power divider (WPD), out–of–phase, 180° coupler, power divider (PD), ultra–wideband (UWB)

Posted Date: July 1st, 2026

DOI: https://doi.org/10.21203/rs.3.rs-10127645/v1

License: This work is licensed under a Creative Commons Attribution 4.0 International License.
Read Full License

Additional Declarations: No competing interests reported.

Systematic Design of Wideband Single-Layer Microstrip 180° Hybrid Couplers Using a Novel Topology

Parisa Safaei* and Masoud Movahhedi**

Abstract – This paper presents two compact wideband microstrip 180° hybrid couplers based on a novel single-layer topology that combines in-phase and out-of-phase power-division techniques. The proposed structures are realized using wideband power dividers and phase-shifting networks, resulting in simple planar implementations with excellent broadband performance. The first hybrid employs a Wilkinson-based architecture, while the second utilizes a novel five-port power divider to further improve compactness and frequency characteristics. Both couplers operate over the 4–9 GHz frequency range and exhibit input return losses better than 12 dB at the Σ and Δ ports. In addition, the simulated isolation between the input ports exceeds 30 dB, while the isolation between the output ports remains better than 15 dB across the entire operating band. The amplitude imbalance is low, and the phase deviation from the desired in-phase and out-of-phase responses is within approximately ±5°. Furthermore, a compact ultra-wideband in-phase power divider with a novel configuration is introduced and incorporated into the proposed hybrid structures. Simulated and measured results show good agreement, confirming the effectiveness of the proposed designs for wideband microwave applications.

Keywords: in–phase; microstrip–slot transition; Wilkinson power divider (WPD); out–of–phase; 180° coupler; power divider (PD); ultra–wideband (UWB).

1. Introduction

180° hybrids, also known as 180° couplers, are fundamental components in microwave and RF systems. They are widely employed in balanced amplifiers, reflectometers, four-port circulators, push–pull power amplifiers, antenna feeding networks, and beamforming systems. By providing in-phase (Σ) and out-of-phase (Δ) signal combinations at their output ports, these devices enable efficient signal splitting and combining while maintaining specific phase relationships between output signals [1].

The growing demand for modern wireless communication, radar, and sensing systems has increased the need for compact and broadband microwave components. Consequently, the design of wideband 180° hybrids with small size, low insertion loss, high isolation, and planar configurations has attracted considerable research interest. Among the available implementations, the conventional rat-race coupler remains one of the most widely used 180° hybrids because of its simple operating principle. However, its bandwidth is inherently limited, and its physical size is relatively large due to the use of fixed quarter-wavelength and three-quarter-wavelength transmission-line sections.

To overcome these limitations, numerous compact and broadband 180° hybrid structures have been reported in the literature. Multi-section and fractal rat-race configurations have been investigated to improve bandwidth and reduce circuit size [2]. Wilkinson-divider-based hybrids have also been proposed to achieve enhanced isolation and broadband performance [3]. Other approaches have utilized microstrip-slotline transitions, ground-slot structures, substrate-integrated technologies, suspended transmission lines, metamaterial-inspired transmission lines, and multilayer implementations [4]–[18]. Although these techniques have demonstrated improved performance in specific aspects, many of them still suffer from one or more drawbacks, including limited bandwidth, fabrication complexity, multilayer configurations, extensive via utilization, non-planar geometries, non-standard impedance requirements, or large phase imbalance.

A common challenge in the design of wideband 180° hybrids is achieving a favorable trade-off among bandwidth,

** Corresponding Author**:** Dept. of Electrical Engineering, Yazd University, Yazd, Iran. (Movahhedi@yazd.ac.ir).

* Dept. of Electrical Engineering, Yazd University, Yazd, Iran.

Received ; Accepted

compactness, fabrication simplicity, and electrical performance. Moreover, many existing structures are developed for a specific implementation and do not provide a generalized framework that can be adapted to different bandwidth and performance requirements.

To address these challenges, this paper presents a novel topology for realizing compact wideband microstrip 180° hybrid couplers. The proposed approach is based on the systematic combination of in-phase power dividers, out-of-phase power dividers, and phase-shifting networks. The main advantage of the proposed topology is its flexibility, which enables the realization of a family of 180° hybrids with different bandwidths and performance characteristics through the appropriate selection of constituent building blocks. Based on this concept, two single-layer wideband microstrip 180° hybrid couplers are designed and implemented. The first structure employs Wilkinson power dividers, whereas the second utilizes a novel five-port power-divider configuration to further improve compactness and frequency response. In addition, a compact ultra-wideband in-phase power divider is introduced and incorporated into the proposed designs. The resulting structures provide wideband operation, good amplitude and phase balance, high isolation, and straightforward fabrication using conventional planar microstrip technology.

The validity of the proposed topology and the performance of the developed couplers are verified through both simulation and experimental measurements. Good agreement between simulated and measured results confirms the effectiveness of the proposed approach.

The remainder of this paper is organized as follows. Section 2 describes the theoretical background, operating principle, and design methodology of the proposed topology and its constituent components. Section 3 presents the design details and experimental results of the proposed 180° hybrid couplers. Finally, Section 4 concludes the paper.

2. Topology of the Proposed 180° Hybrid Couplers

The operating principle of the proposed 180° hybrid couplers can be described using the scattering matrix given in (1). According to this matrix, when α = β, the incident power at any excitation port is equally divided between two output ports, while the remaining ports remain matched.

$$S = \begin{bmatrix} 0 & \alpha & \beta & 0 \\ \alpha & 0 & 0 & -\beta \\ \beta & 0 & 0 & \alpha \\ 0 & -\beta & \alpha & 0 \end{bmatrix} \quad (1)$$

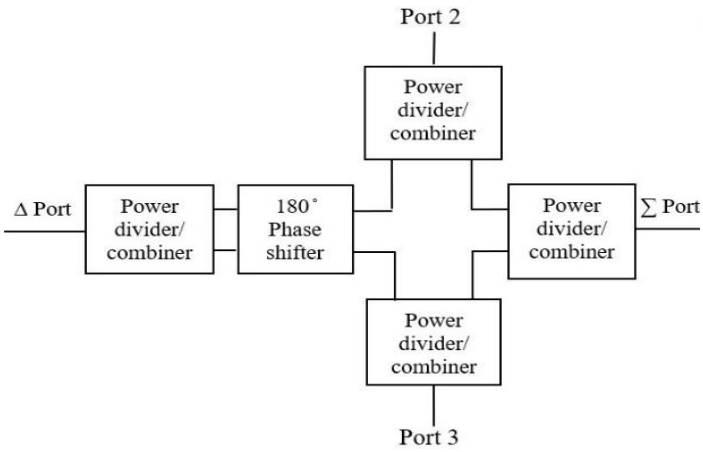


Fig. 1. Block diagram of proposed wideband 180° coupler [20].

It should be noted that the phase relationship between the output signals depends on the selected excitation port. When port 1 is excited, the signals appearing at the output ports are in phase. In contrast, excitation of port 4 results in two output signals with a phase difference of 180°. Furthermore, when signals are simultaneously applied to ports 2 and 3, port 1 provides the sum (Σ) of the two signals, whereas port 4 provides their difference (Δ). Consequently, ports 1 and 4 are conventionally referred to as the Σ and Δ ports, respectively. As with any ideal hybrid coupler, the device is lossless, reciprocal, and perfectly matched.

The conceptual block diagram of the proposed topology is shown in Fig. 1 [20]. The structure consists of a four-port 180° phase shifter and four in-phase power dividers. An in-phase power divider equally splits an input signal into two signals of identical amplitude and phase, whereas the 180° phase shifter converts two arbitrary input signals into two output signals with a phase difference of 180°.

The proposed topology provides a generalized framework for the realization of a wide range of 180° hybrid couplers. By appropriately selecting the constituent power dividers and phase-shifting networks, couplers with different bandwidths and performance characteristics can be obtained while preserving the same fundamental operating principle. Owing to the symmetry and signal-flow characteristics of the topology, all couplers derived from the block diagram of Fig. 1 exhibit the scattering matrix given by

$$S = (-j/2)\begin{bmatrix} 0 & 1 & 1 & 0 \\ 1 & 0 & 0 & -1 \\ 1 & 0 & 0 & 1 \\ 0 & -1 & 1 & 0 \end{bmatrix} \quad (2)$$

This matrix indicates that the proposed hybrid inherently provides equal power division between the output ports, corresponding to a coupling level of 3 dB (−6 dB transmission coefficient magnitude).

Since the output ports are not symmetrically positioned with respect to the excitation ports, conventional even–odd mode analysis cannot be directly applied. Therefore, a matrix reduction approach suitable for asymmetric multi-port networks is employed. To investigate the relationship between ports 2 and 4, ports 1 and 3 are terminated with short circuits ($Z_L = 0$), reducing the original four-port network to an equivalent two-port structure. Under these conditions, the load reflection matrix can be written as:

$$\Gamma_L = \begin{bmatrix} \Gamma_{L3} & 0 \\ 0 & \Gamma_{L1} \end{bmatrix} = \begin{bmatrix} -1 & 0 \\ 0 & -1 \end{bmatrix} \tag{3}$$

Using the matrix reduction procedure described in [23] and [24], the reduced scattering parameters are obtained from:

$$\acute{S}_{ij} = S_{ij} + \frac{\Gamma_{L3}\begin{vmatrix} S_{i3}S_{3j} & -S_{i3}S_{31}\Gamma_{L1} \\ S_{1j} & 1 - S_{11}\Gamma_{L1} \end{vmatrix} + \Gamma_{L1}\begin{vmatrix} S_{3j} & 1 - S_{33}\Gamma_{L3} \\ -S_{i1}S_{1j} & S_{i1}S_{13}\Gamma_{L3} \end{vmatrix}}{\begin{vmatrix} 1 - S_{33}\Gamma_{L3} & -S_{31}\Gamma_{L1} \\ -S_{13}\Gamma_{L3} & 1 - S_{11}\Gamma_{L1} \end{vmatrix}}$$
$$for\ i,j = 2,4 \tag{4}$$

where $\acute{S}_{ij}$ represents the elements of the reduced two-port scattering matrix. Substituting the scattering parameters of the ideal hybrid into (4) yields

$$\acute{S}_{24} = \begin{bmatrix} \frac{2}{10} & \frac{6}{10}j \\ \frac{6}{10}j & \frac{2}{10} \end{bmatrix} \tag{5}$$

The reduced matrix in (5) predicts the expected values of S_{22}, S_{24}, S_{42}, and S_{44}. As will be demonstrated in Section 3, the measured results of both proposed couplers closely agree with these theoretical predictions, thereby validating the proposed topology.

A similar procedure can be applied to ports 3 and 4. By short-circuiting ports 1 and 2, the corresponding reduced scattering matrix becomes

$$\acute{S}_{34} = \begin{bmatrix} \frac{2}{10} & -\frac{6}{10}j \\ -\frac{6}{10}j & \frac{2}{10} \end{bmatrix} \tag{6}$$

Comparison of (5) and (6) reveals that equal power is delivered from port 4 to ports 2 and 3, while the transmitted signals exhibit a phase difference of 180°. The experimental results presented later confirm this behavior and demonstrate excellent agreement with the theoretical analysis. Similar reduced matrices may also be derived for the remaining port combinations.

The operating mechanism of the proposed hybrid can be readily understood from the signal-flow diagram of Fig. 1. When the Δ port is excited, the input signal is first equally divided into two signals with identical amplitude and phase. These signals subsequently pass through the 180° phase shifter, producing two signals of equal magnitude but opposite phase. The resulting signals are delivered to ports 2 and 3. Any signal components propagating toward the Σ port combine destructively because of their equal amplitudes and 180° phase difference, leading to complete cancellation. Consequently, the Σ port is isolated from the Δ port.

Similarly, when the Σ port is excited, the interconnected power dividers form an equivalent in-phase power-division network. The incident signal is equally distributed between ports 2 and 3 with identical amplitude and phase. Any signal components propagating toward the Δ port experience destructive interference because half of the signal paths introduce a 180° phase reversal. As a result, the net signal at the Δ port becomes zero, ensuring isolation between the Σ and Δ ports.

Therefore, the proposed topology simultaneously provides in-phase and out-of-phase power division while maintaining high isolation between the Σ and Δ ports, which constitutes the fundamental operating principle of the proposed 180° hybrid couplers.

3. Design and Analysis of Proposed 180° Hybrids

This section presents two practical implementations of the proposed 180° hybrid topology. Both couplers are realized using planar microstrip technology and are designed to provide wideband operation, compact size, good amplitude balance, and accurate phase performance. Although the two structures share the same theoretical foundation described in Section II, they differ in the realization of the power-division network. The first design employs Wilkinson power dividers and a wideband phase-shifting section, whereas the second design incorporates a novel five-port power divider based on parallel microstrip lines to further improve compactness and bandwidth characteristics. Detailed design procedures and performance evaluations of the proposed couplers are provided in the following subsections.

3.1 Design and Results of the First 180° Hybrid Coupler (Work I)

The first proposed 180° hybrid coupler is developed based on the topology introduced in Section II. Prior to presenting the complete hybrid structure, the constituent building blocks, namely the ultra-wideband (UWB) out-of-phase and in-phase power dividers, are briefly reviewed. As illustrated in Fig. 2, an out-of-phase power divider can be realized by combining a suitable power divider with a 180° phase-

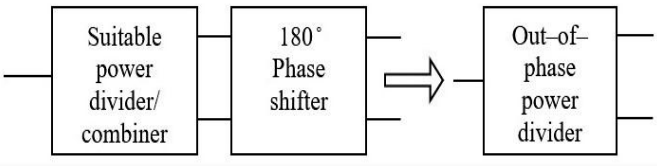


Fig. 2. Out–of–phase power divider resulting from the connection of a suitable power divider and a 180° phase shifter.

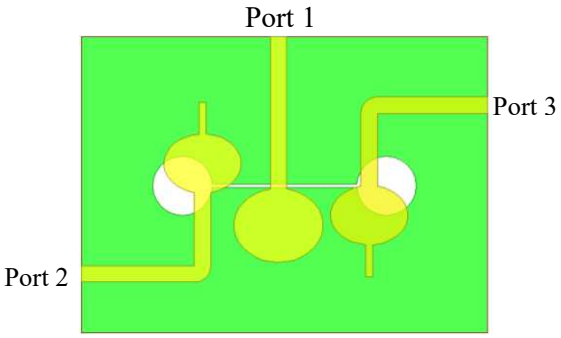
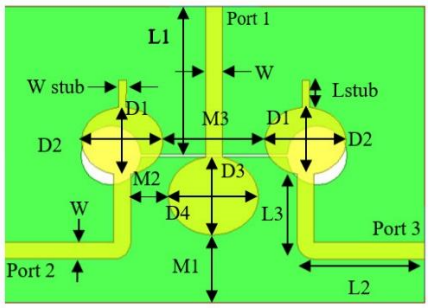
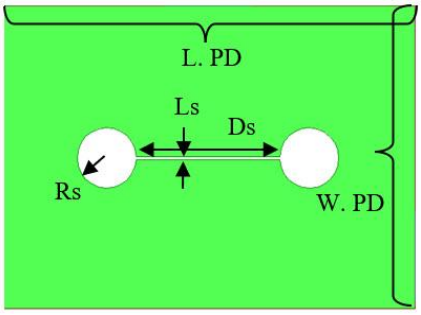


Fig. 3. Compact UWB out–of–phase power divider [21].



(a)



(b)

Fig. 4. Compact UWB in–phase power divider used in 180° hybrid. (a) top. (b) bottom.

shifting network. To implement this function, the compact single-layer structure reported in [21], shown in Fig. 3, is employed. All ports are located on the top metallization layer, whereas the ground plane is placed on the opposite side of the substrate.

The in-phase power divider used in the proposed hybrid is shown in Fig. 4. This divider features a compact planar

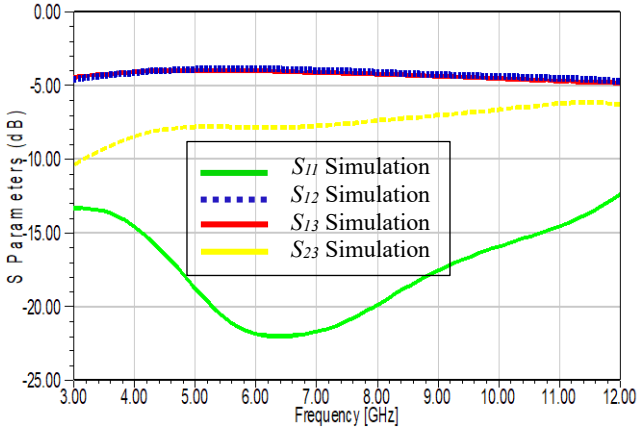


Fig. 5. Frequency response of the in–phase power divider.

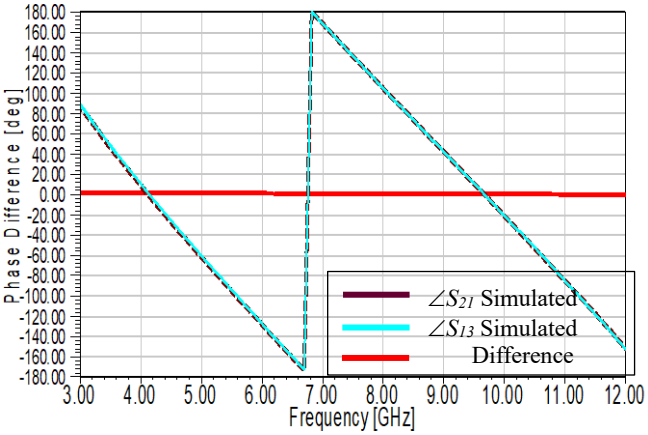
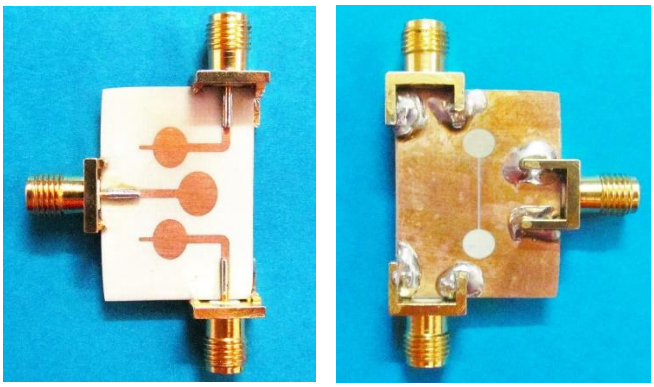


Fig. 6. Phase characteristics of the in–phase power divider.



(a) (b)

Fig. 7. Proposed fabricated in–phase power divider. (a) top layer. (b) bottom layer.

configuration, ultra-wideband operation, and a single-layer implementation. The structure consists of microstrip-to-slotline transitions without requiring any resistive elements. Owing to its symmetrical geometry, the input signal is equally divided into two output signals with identical amplitude and phase. The ground plane incorporates a rectangular slot connected to two circular slots, while elliptical patches are introduced on one side of the microstrip

lines to improve impedance matching and bandwidth performance. The simulated frequency and phase responses of the divider are presented in Figs. 5 and 6, respectively, whereas the fabricated prototype with a compact size of *28 mm × 20 mm* is shown in Fig. 7.

Compared with the design presented in [20], the proposed coupler achieves a more compact and simplified implementation by eliminating the additional substrate layer and reducing the overall footprint. Furthermore, all four ports are positioned on a single metallization layer, resulting in a fully planar single-layer microstrip structure. This configuration not only simplifies the fabrication process but also improves compatibility with conventional planar microwave circuits and integrated front-end systems.

The complete 180° hybrid coupler is realized by combining the out-of-phase power divider, the proposed in-phase power divider, and two Wilkinson power dividers (WPDs), as shown in Fig. 8. Compared with the previously reported structure in [20], the proposed design eliminates the additional substrate layer and achieves a fully planar configuration with all four ports located on the same metallization layer. This feature significantly simplifies fabrication and facilitates integration with conventional microstrip circuits.

When port Δ is excited, the signal is first coupled to the slotline through a microstrip-to-slotline transition and subsequently divided into two equal-magnitude signals with a 180° phase difference. After passing through the Wilkinson power dividers, the signals are delivered to ports 2 and 3. Due to the equal amplitudes and opposite phases of the signal components propagating toward port Σ, destructive interference occurs, resulting in high isolation between ports Δ and Σ. Similarly, when port Σ is excited, the combination of the in-phase power divider and the Wilkinson power divider operateس as an equivalent in-phase power division network. Consequently, the input signal is equally distributed between ports 2 and 3 while maintaining identical phase characteristics. Under these conditions, destructive interference suppresses signal transmission toward port Δ, thereby ensuring isolation between the sum and difference ports. The electric-field distributions under Σ-port and Δ-port excitations are shown in Fig. 9, confirming the proposed operating mechanism and the isolation between the two input ports.

Although the proposed coupler was primarily designed and optimized using full-wave electromagnetic simulations, several design guidelines can be provided to facilitate the initial implementation. The slotline width was selected to achieve proper impedance matching according to the

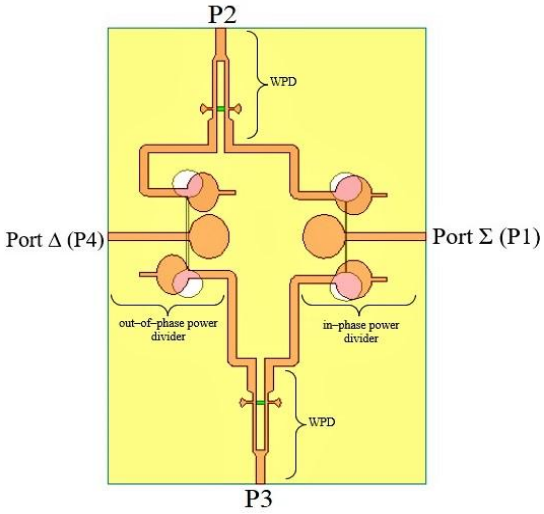


Fig. 8. Proposed wideband 180° hybrid.

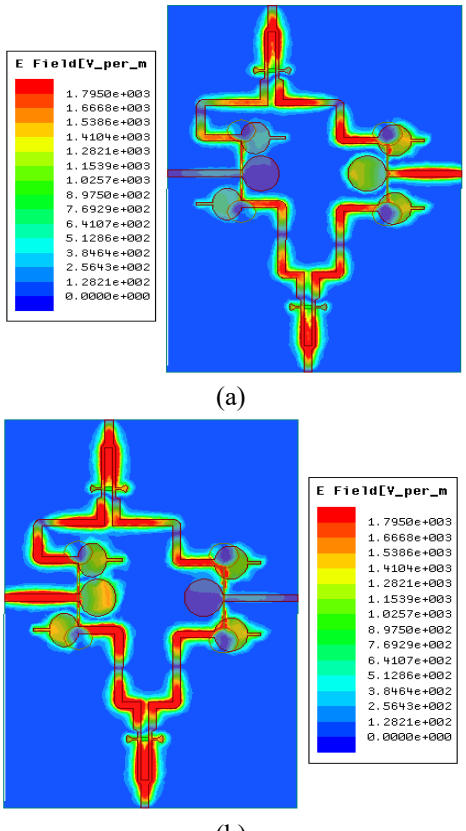
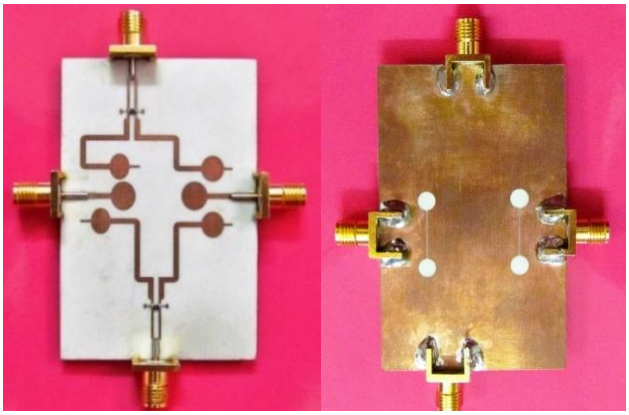


Fig. 9. The E–field distribution of the proposed 180˚ coupler. (a) Port Σ excitation. (b) Port Δ excitation.

procedures described in [6] and [7], where the slotline characteristic impedance was assumed to be approximately $2Z_0 \cong 120\ \Omega$. In addition, the slotline length was chosen to be λg/4 at the center frequency ($f_c = 6.8\,GHz$), which can be estimated from $d = \frac{c}{4f_c\sqrt{\varepsilon_{re}}}$ where $\varepsilon_{re} = \frac{\varepsilon_r+1}{2}$ denotes the effective dielectric constant.



(a) (b)

Fig. 10. Proposed fabricated 180˚ coupler. (a) top layer. (b) bottom layer.

TABLE I
Optimized Values of The First 180˚ Hybrid.

Parameter	Values (mm)
W	1.11687
L1	10.18
L2	8.5
L3	5.7
D 1	4.6
D2	5.4
L stub	1.83
W stub	0.5
D3	5.28
D4	6
Ls	9.72
Ds	0.2
Rs	2
M1	4.56
M2	2.51
M3	6.82
L. PD	28
W. PD	20

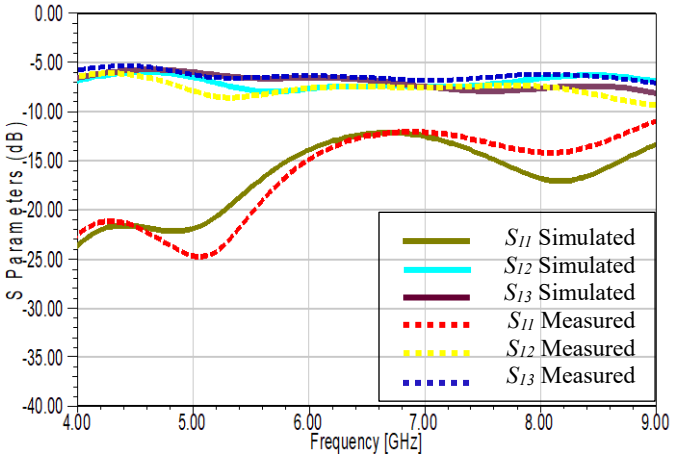


Fig. 11. Frequency responses of port Δ.

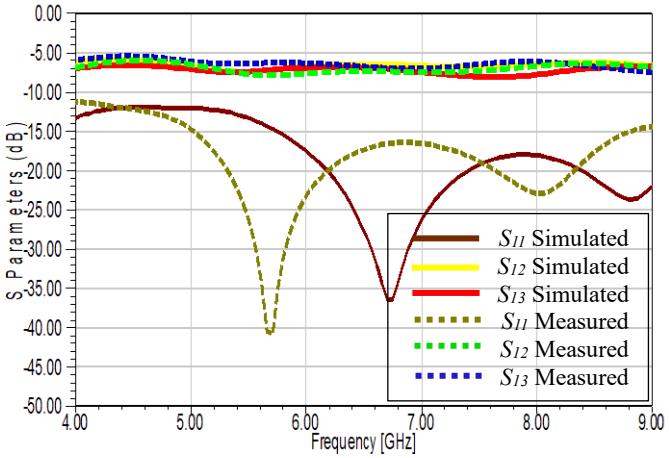


Fig. 12. Frequency responses of port ∑.

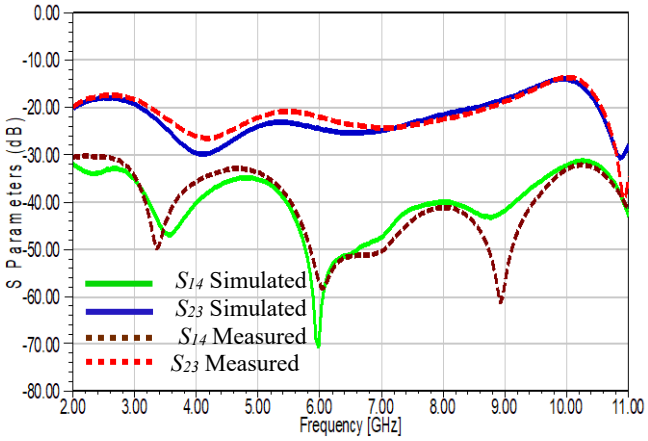


Fig. 13. Isolation between different ports.

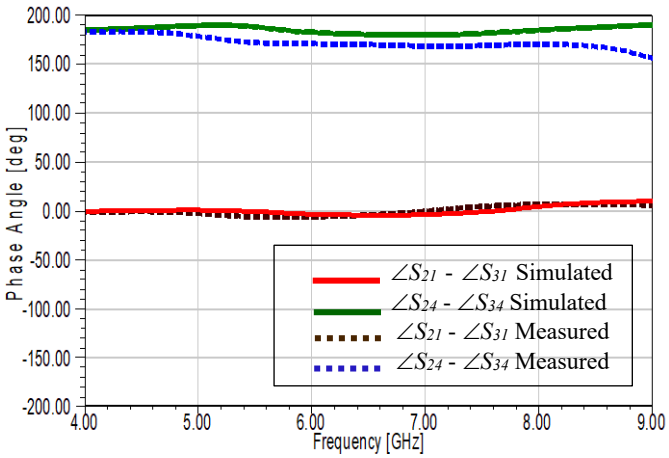


Fig. 14. Phase differences of the proposed structure.

The fabricated prototype of the proposed single-layer 180° hybrid coupler is shown in Fig. 10. The overall dimensions of the structure are *35 mm* × *60 mm*, while the optimized design parameters are listed in Table I. The design and optimization process was carried out using Ansoft HFSS. Rogers RO4003C substrate with a dielectric constant of 3.38, loss tangent of 0.0027, and thickness of 0.508 mm was

employed for both simulation and fabrication.

The simulated and measured responses of the Δ port are presented in Fig. 11. Good agreement is observed between the simulated and measured results. The measured return loss (S_{44}) remains better than 10 dB over the frequency range of 4–9 GHz. Moreover, the measured transmission coefficients from port Δ to ports 2 and 3 are approximately -8 dB and -7 dB, respectively, resulting in an amplitude imbalance of about ±1 dB across the operating band.

The performance of the Σ port is shown in Fig. 12. The measured return loss is better than 10 dB from 3 to 10.5 GHz. Furthermore, the measured transmission coefficients from port Σ to ports 2 and 3 are approximately 6 dB with less than ±0.5 dB amplitude imbalance over the 4–9 GHz frequency range. The measured isolation characteristics are illustrated in Fig. 13. The isolation between ports Σ and Δ (S_{14}) exceeds 30 dB from 2 to 11 GHz, while the measured isolation between output ports (S_{23}) remains better than 15 dB over the same frequency range.

Fig. 14 compares the simulated and measured phase responses of the proposed coupler. The measured phase difference between ports 2 and 3 is maintained within 180° ± 10° under Δ-port excitation and within 0° ± 5° under Σ-port excitation throughout the 4–9 GHz operating band, confirming the proper out-of-phase and in-phase characteristics of the proposed hybrid.

3.2 Design and Results of the Second 180° Hybrid Coupler (Work II)

The second 180° hybrid coupler was developed to further reduce the circuit size while improving the frequency performance of the first design. Similar to Work I, the proposed structure is derived from the topology presented in Fig. 1. However, in this implementation, the Wilkinson power dividers are replaced by a novel five-port power-divider configuration based on parallel microstrip lines, resulting in a more compact and fully planar structure.

The geometry of the proposed coupler and the corresponding five-port power divider are shown in Fig. 15(a) and Fig. 15(b), respectively. The compact ultra-wideband out-of-phase power divider reported in [21] is employed to realize the out-of-phase power division because of its favorable bandwidth characteristics and compact size. In addition, a rectangular slot is etched in the ground plane to provide electromagnetic coupling among ports Σ, 2, and 3.

The in-phase power-division section consists of a five-port structure formed by parallel microstrip lines. To improve impedance matching and coupling performance, six rectangular stubs are incorporated into the microstrip lines. The dimensions and locations of these stubs were determined

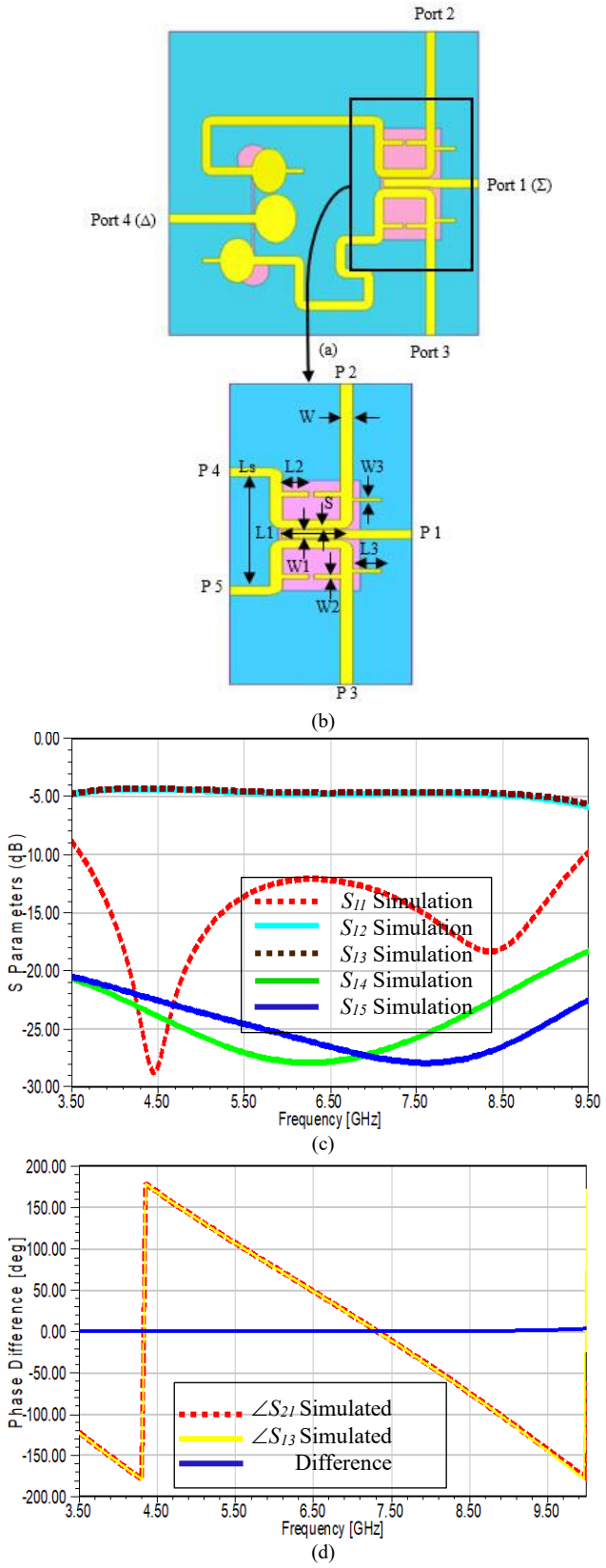


Fig. 15. (a) The 180˚ coupler using out–of–phase power divider and parallel microstrip lines. (b) The five–port structure. (c) Frequency response of the five–port power divider. (d) Phase characteristics of the five–port power divider.

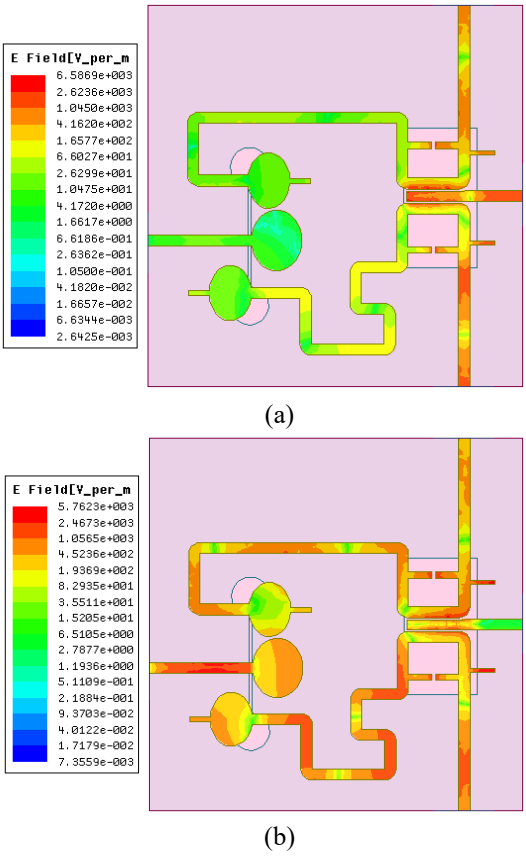


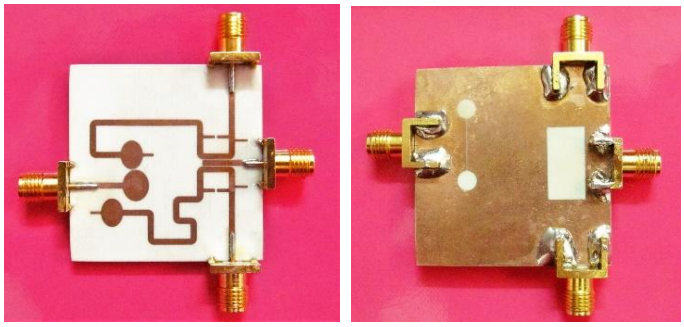
Fig. 16. E–field distribution of the proposed 180˚ coupler. (a) Port Σ excitation. (b) Port Δ excitation.

TABLE II
Optimized Values of The Second 180˚ Hybrid.

Parameter	Values (mm)
W	1.11687
L 1	5
W1	1
L2	2.3
W2	0.6
L3	2.5
W3	0.4
Ls	13.65
s	0.2

through full-wave optimization. Owing to the symmetrical configuration of the structure, equal power division between ports 2 and 3 is achieved while maintaining the operating characteristics predicted by the theoretical analysis presented in Section II.

The simulated frequency and phase responses of the proposed five-port power divider are presented in Figs. 15(c) and 15(d), respectively. Furthermore, the electric-field distributions under Σ-port and Δ-port excitations are illustrated in Fig. 16. The field distributions confirm the



(a) (b)

Fig. 17. Proposed fabricated compact 180˚ hybrid. (a) top layer. (b) bottom layer.

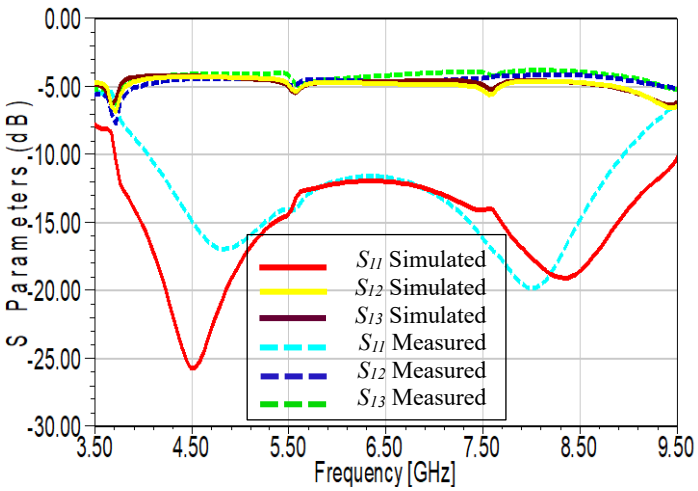


Fig. 18. Frequency responses of port ∑.

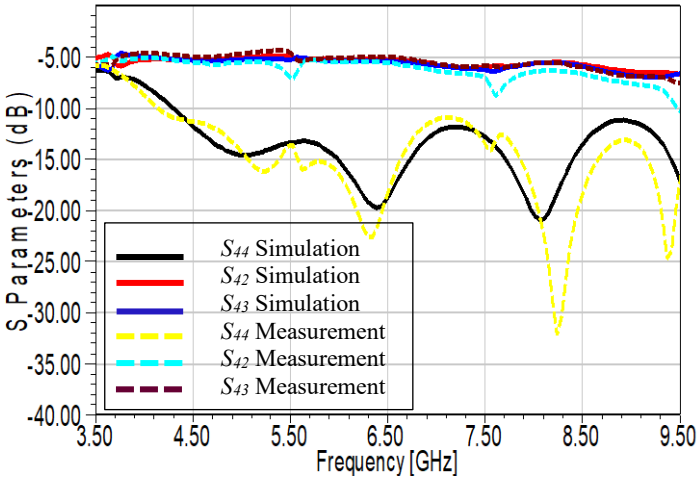


Fig. 19. Frequency responses of port Δ.

operating mechanism of the proposed hybrid and demonstrate the high isolation between the Σ and Δ ports. They also highlight the roles of the rectangular stubs and ground-plane slot in controlling the signal propagation and coupling characteristics.

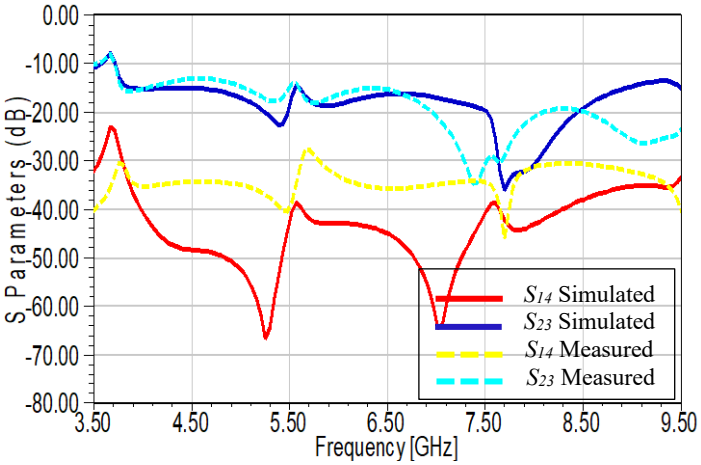


Fig. 20. Isolation between different ports.

The coupler was designed and optimized using Ansoft HFSS on a Rogers RO4003C substrate with a dielectric constant of 3.38, loss tangent of 0.0027, and thickness of 0.508 mm. The optimized design parameters are listed in Table II. A photograph of the fabricated prototype is shown in Fig. 17. The overall dimensions of the coupler are 37.6 mm × 37 mm, representing a substantial reduction in footprint compared with the first design while preserving a single-layer planar configuration.

The simulated and measured responses of the Σ port are presented in Fig. 18. Good agreement is observed between simulation and measurement results. The measured return loss of port Σ remains better than 10 dB over the frequency range of 3.8–9 GHz. In addition, the measured transmission coefficients from port Σ to ports 2 and 3 are approximately equal across the operating band, resulting in an amplitude imbalance of less than 0.5 dB.

Figure 19 shows the simulated and measured responses of port Δ. The measured return loss (S_{44}) is better than 10 dB from 4 to 9.5 GHz. Moreover, the measured transmission coefficients from port Δ to ports 2 and 3 vary between approximately 5 dB and 6 dB over the 4–9 GHz frequency range, corresponding to an amplitude imbalance of about 1 dB.

The measured isolation characteristics are shown in Fig. 20. The isolation between the Σ and Δ ports (S_{14}) exceeds 30 dB from 4 to 9.5 GHz, while the measured isolation between output ports (S_{23}) remains better than 15 dB throughout the operating band. These results confirm the effectiveness of the proposed topology in maintaining high port isolation over a wide frequency range.

The simulated and measured phase responses of the coupler are compared in Fig. 21. The measured phase difference between ports 2 and 3 remains within 180° ± 5° under Δ-port excitation and within 0° ± 5° under Σ-port excitation from 4 to 9 GHz. These results verify the accurate realization of both

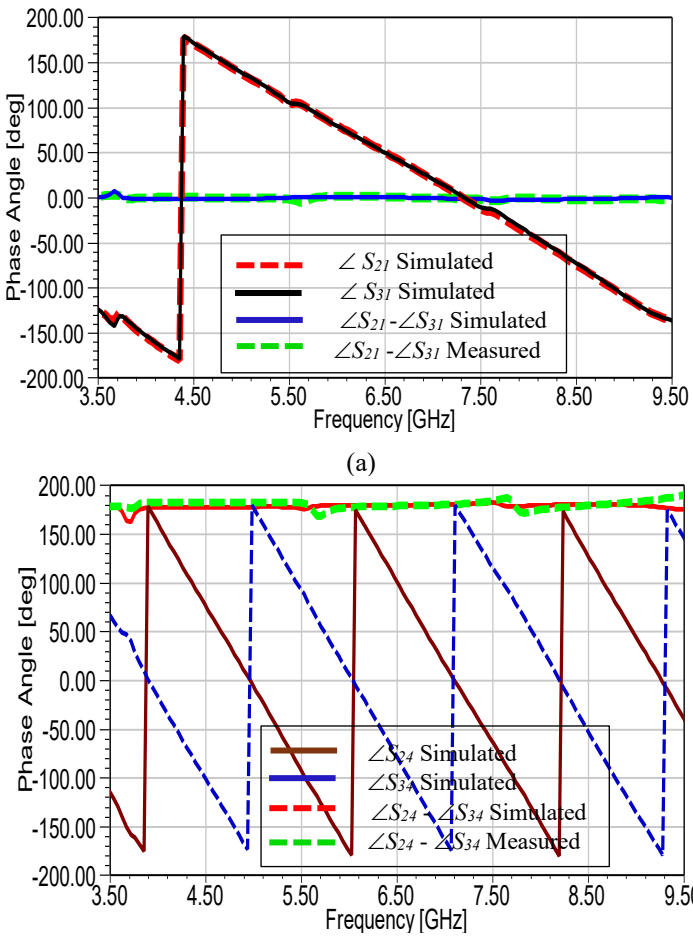


Fig. 21. Phase differences of the proposed structure. (a) In–phase excitation. (b) out–of–phase excitation.

out-of-phase and in-phase power division and demonstrate the excellent phase balance of the proposed hybrid coupler.

The transition from Work I to Work II demonstrates the design flexibility offered by the proposed topology. By replacing the Wilkinson power dividers with the compact five-port power-divider configuration, the occupied area was reduced by approximately 34%, while the measured fractional bandwidth increased from 73% to 87%. Furthermore, the second design preserved the desirable characteristics of the first coupler, including low amplitude imbalance, accurate phase performance, and high isolation between the Σ and Δ ports. These improvements verify that the proposed topology can be effectively adapted to achieve different trade-offs between size and frequency performance without altering its fundamental operating principle.

Finally, Table III compares the performance of the proposed couplers with previously reported 180° hybrid structures. The comparison indicates that the proposed designs provide a favorable combination of wide bandwidth, compact size, planar implementation, and fabrication simplicity. In

TABLE III
Comparison of 180° Couplers.

Reference	[15]	[16]	[17]	[22]	[23]	**Work I**	**Work II**
Freq. Bands (GHz)	0.66-3.34	0.6-1	3-5	22-26	1.7-2.3	**4-9**	**3.5-9.5**
f_0 (GHz)	2	0.8	4	24	2	**6.8**	**6.8**
FBW (%)	134	50	50	16	32	**73**	**87**
RL (dB)	10	10	20	15	10	**12**	**12**
Physical Size (mm^2)	$\cong 90 * 40$	$\cong 42 * 67$	$\cong 42 * 67$	$\cong 40 * 42$	$\cong 40.4 * 62.2$	**35 * 60**	**37.5*37**
Normalized Size	$0.60\lambda_o \times 0.27\lambda_o$	$0.11\lambda_o \times 0.18\lambda_o$	$0.56\lambda_o \times 0.89\lambda_o$	$3.20\lambda_o \times 3.36\lambda_o$	$0.27\lambda_o \times 0.41\lambda_o$	$\mathbf{0.79\lambda_o \times 1.36\lambda_o}$	$\mathbf{0.85\lambda_o \times 0.84\lambda_o}$
Configuration	3D Structure-Non-planar-2 Section	1 Layer	1 Layer	Complicated-Multi-layers-Planar	Planar-1 Layer	**Simple-Planar-1 Layer**	**Simple-Planar-1 Layer**

particular, both couplers achieve broadband operation using a single-layer microstrip configuration without requiring multilayer structures, suspended substrates, or extensive via interconnections, making them attractive candidates for modern microwave and RF front-end applications.

4. Conclusion

This paper presented a novel topology for the realization of compact wideband microstrip 180° hybrid couplers. The proposed approach is based on the systematic combination of in-phase power dividers, out-of-phase power dividers, and phase-shifting networks, providing a flexible framework for developing 180° hybrids with different performance characteristics and bandwidth requirements.

To validate the proposed concept, two single-layer microstrip 180° hybrid couplers were designed, fabricated, and experimentally characterized. The first design employed Wilkinson power dividers, whereas the second utilized a novel five-port power-divider configuration to further improve compactness and bandwidth performance. Both couplers exhibited wideband operation, good amplitude and phase balance, and high isolation between the Σ and Δ ports. The measured results showed good agreement with the full-wave simulations, confirming the validity of the proposed topology and design methodology.

In addition, a compact ultra-wideband in-phase power divider was developed and successfully incorporated into the proposed structures. The experimental results demonstrated that the proposed couplers achieve broadband performance while maintaining a simple single-layer planar configuration, making them suitable for integration into modern microwave and RF front-end systems. The flexibility of the proposed topology also provides a practical foundation for the development of future wideband 180° hybrid couplers with customized performance requirements.

References

[1] D. M. Pozar, *Microwave Engineering*, 4th ed, New York, USA: Wiley, 2005, ch. 7, pp. 362.

[2] M. Caillet, M. Clénet, A. Sharaiha and Y. M. M. Antar, "A compact wide–band rat–race hybrid using microstrip lines,'' *IEEE Microw. Wireless Compon Lett,* vol. 19, no. 4, pp. 191–193, Apr. 2009. DOI: 10.1109/LMWC.2009.2015483.

[3] N. Yang, C. Caloz, and K. Wu, "Broadband compact 180 hybrid derived from the Wilkinson divider," *IEEE Trans. Microw. Theory Tech.,* vol. 58, no. 4, pp. 1030–1037, Apr. 2010. DOI: 10.1109/TMTT.2010.2042631.

[4] B. Henin and A. Abbosh, "Wideband hybrid using three–line coupled structure and microstrip–slot transitions," *IEEE Microw. Wireless Compon. Lett.*, vol. 23, no. 7, Jul. 2013. DOI: 10.1109/LMWC.2013.2262930.

[5] O. Ahmed and A. R. Sebak, "A modified Wilkinson power divider/combiner for ultrawideband communications," *Antennas and Propag. Society Int. Symp.,* Jun. 2009. DOI: 10.1109/APS.2009.5171657.

[6] B. Schuppert, "Microstrip/slot line transitions: Modeling and experimental investigation," *IEEE Trans. Microw. Theory*

Tech., vol. MTT–36, no. 8, pp. 1272–1282, Aug. 1988. DOI: 10.1109/22.3669.

[7] J. Knorr, "Slot–line transitions," *IEEE Trans. Microw. Theory Tech*., vol. MTT–22, pp. 548–554, May. 1974. DOI: 10.1109/TMTT.1974.1128278.

[8] M. Bialkowski and Y. Wang, "Wideband microstrip 180˚ hybrid utilizing ground slots," *IEEE Microw. Wireless Compon. Lett.*, vol. 20, no. 9, pp. 495–497, Sep. 2010. DOI: 10.1109/LMWC.2010.2056677.

[9] R. Nakano, T. Kawai and A. Enokihara, "76 GHz band rat–race circuit utilizing composite right–/left–handed transmission line without Chip Elements," *12th. German Microw. Conf., (GeMiC),* 2019. DOI: 10.23919/GEMIC.2019.8698195.

[10] R. Smolarz, K. Wincza and S. Gruszczynski, "Broadband rat–race coupler in suspended stripline technique for measurements of large–signal S parameters," *21st Int. Conf. Microw, Radar. Wireless Commun. (MIKON)*, May. 2016. DOI: 10.1109/MIKON.2016.7492082.

[11] B. D. Nguyen, M. T. Vu and M. L. Nguyen, "A multi-layer design of 3-dB 180˚ wideband hybrid coupler," *IEEE Int. Conf. Computational Electrom (ICCEM)*, Aug. 2020. DOI: 10.1109/ICCEM47450.2020.9219511.

[12] C. H. Chi and C. Y. Chang, "A New Class of Wideband Multisection 180° Hybrid Rings Using Vertically Installed Planar Couplers," *IEEE Trans. Microw. Theory Tech.,* vol. 54, no. 6, pp. 2478 - 2486, Jun. 2006. DOI: 10.1109/TMTT.2006.875799.

[13] C. Pfeiffer, T. Steffen and B. Tomasic, "UWB Millimeter-Wave 180° Hybid Couplers," *IEEE Int. Symp. Antennas Propag. USNC-URSI Radio Science Meeting,* Jul. 2019. DOI: 10.1109/APUSNCURSINRSM.2019.8889228.

[14] B. Zhou, X. Li, C. Li, L. Qian and Z. Cai, "Broadband 180° hybrid for 5G applications," *IEEE CPMT, Symp, Japan (ICSJ).,* Nov. 2019. DOI: 10.1109/ICSJ47124.2019.8998710.

[15] Ao. Li, and K-M. Luk, "Millimeter-wave dual linearly polarized endfire antenna fed by 180° hybrid coupler," *IEEE Antennas. Wireless. Propag. Lett*., vol. 18, no. 7, pp. 1390 – 1394, Jul. 2019. DOI: 10.1109/LAWP.2019.2917660.

[16] K. V. P. Kumar, R. K. Barik, I. S. Krishna and S. S. Karthikeyan, "Design of compact 180° hybrid coupler for unequal power division ratio using slow wave structures," *Twenty-third National Conf. Commun. (NCC),* 2017. DOI: 10.1109/NCC.2017.8077127.

[17] Y. Ma, K. Ma and Y. Wang, "A Novel 180° Coupler Based on Double-sided Substrate Integrated Suspended Line Technology with Patterned Substrate," *48th European Microw. Conf. (EuMC),* 2018. DOI: 10.23919/EuMC.2018.8541649.

[18] P. Li, H. Ren, Y. Gu, B. Pejcinovic and B. Arigong, "A Second Harmonic Separation Symmetric Ports 180° Coupler with Arbitrary Coupling Ratio and Transparent Terminations," *IEEE/MTT-S International Microwave Symposium (IMS),* 2020. DOI: 10.1109/IMS30576.2020.9223777.

[19] K. S. Ang and Y. C. Leong, "Converting baluns into broad-band impedance-transforming 180_ hybrids," *IEEE Trans. Microw. Theory Tech.*, vol. 50, no. 8, pp. 1990_1995, Aug. 2002. DOI: 10.1109/TMTT.2002.801353.

[20] P. Safaie, M. Movahhedi and A. G. Yazdi, "A systematic method to design desired wideband 180° couplers," *27th Iranian Conf. Elect. Eng. (ICEE)*, Yazd, Iran, Apr. 2019. DOI: 10.1109/Iranian CEE.2019.8786520.

[21] P. Safaei and M. Movahhedi, "A compact UWB single–layer out–of–phase power divider based on microstrip–slot line transitions," *AUT Journal. Elect. Eng (AUTJEE)*, 2021. DOI: 10.22060/EEJ.2021.19912.5412. in Press.

[22] L. Guo and A. Abbosh, "Phase shifters with wide range of phase and ultra–wideband performance using stub–loaded coupled structure," *IEEE Microw. Wireless Compon. Lett.*, vol. 24, no. 3, Mar. 2014. DOI: 10.1109/LMWC.2013.2293658.

[23] R. Sinha, "Synthesis of asymmetric multiport network," Ph.D. dissertation, *Dept. Electron. Elect. Commun. Eng.*, Institute of Technology., Kharagpur. India. 2016.

[24] T.Y. Otoshi, "On the scattering parameters of a reduced multiport," *IEEE Trans. Microw. Theory Tech*., Vol: 17, no. 9, pp. 722 – 724, Sep. 1969. DOI: 10.1109/TMTT.1969.1127045.